Computational modeling for cell spreading on a substrate mediated by specific interactions, long-range recruiting interactions, and diffusion of binders

Lu Sun,[1] Qian Hua Cheng,[2] H. J. Gao,[3] and Yong-Wei Zhang[1,2,*]
[1]*Department of Materials Science and Engineering, National University of Singapore, Singapore 119260, Singapore*
[2]*Institute of High Performance Computing, A*Star, Singapore 138632, Singapore*
[3]*Division of Engineering, Brown University, Providence, Rhode Island 02912, USA*
(Received 3 October 2008; revised manuscript received 28 April 2009; published 5 June 2009)

A continuum model was proposed to study cell spreading on a flat substrate mediated by specific interaction, long-range recruiting interaction, and the diffusion of binders. Specific interactions between the mobile receptors embedded in the cell membrane and ligands coated on the substrate surface result in cell adhesion to the substrate surface. This receptor-ligand interaction was described by a chemical reaction equation. Long-range recruiting interactions between the receptors and the substrate were simplified by a traction-separation law. The governing equations and boundary conditions were formulated for the entire process of cell spreading and solved using a finite element scheme. Parametric studies were conducted to investigate the effect of system parameters on the cell spreading kinetics. It is shown that kinetic factors play an important role in cell adhesion and three regimes, that is, the binder reaction limited regime, long-range recruiting force-driven binder recruitment limited regime, and the concentration gradient-driven diffusion limited regime, were identified.

DOI: 10.1103/PhysRevE.79.061907 PACS number(s): 87.17.Aa, 87.17.Rt, 87.15.A−, 87.15.hg

I. INTRODUCTION

The adhesion of cells to the extracellular matrix (ECM) plays a crucial role in dynamic biological processes, for example, embryo growing, cancer metastasis, tissue regeneration, and inflammatory response [1,2]. A weakly bound state is initiated by relatively weak nonspecific forces such as attractive van der Waals forces and repulsive steric forces. Subsequently, a strongly bound state is then mediated by the specific interactions between surface proteins called receptor and ligand [3,4]. It was shown that at molecular level, this specific interaction serves as a stimulus for a complex cascade of signaling events [5], which subsequently triggers remodelling of cytoskeleton, resulting in contractile force generations and cellular morphological changes [6].

Since the time scale for active cytoskeletal remodeling to occur is over minutes, the cell adhesion dominated by physical properties is at much shorter time scale than the above time scale [7]. It was also observed that cells are capable of exerting significant forces before actin polymerization or visible stress fiber formation [8]. Therefore, in biomimetic systems which are devoid of cytoskeleton, the complexity of cytoskeletal rearrangement or intracellular signals can be avoided, while important insights into cell adhesion can be still gained by studying the passive spreading process [9].

A number of theoretical frameworks have been proposed by assuming the dominance of physical process in cell adhesion. After the general thermodynamic framework proposed in [3,4], it was commonly accepted that cell adhesion is mediated by receptor-ligand interactions. The process of cell adhesion or deadhesion from a substrate tissue was subsequently modeled by adopting a traditional cohesive zone model [10]. However, cell adhesion is a nonequilibrium process, upon which several kinetic models have been established subsequently. For example, a chemical reaction rate theory was applied to describe the interaction between receptors and ligands. Based on receptor diffusion and binding and unbinding reaction, biomimetic systems such as large synthetic vesicles were studied [11]. It was suggested that the transient nature of cell spreading can be either binder diffusion limited or binder chemical reaction limited [11,12].

Although the adhering models of cell have been extensively studied at the cellular scale and considerable advance has been achieved, several issues are still in need of in-depth understanding. First, the individual effects of specific interactions and long-range recruiting interactions on cell adhesion have been poorly differentiated in the existing theoretical models on cell adhesion. Considering the marked difference in their interaction strength and length scales, it is expected that specific interactions and long-range recruiting forces play different roles in regulating cell adhesion. Second, the binding and rupture kinetics of a collection of receptor-ligand bonds were found to be affected by several parameters, for example, interfacial stress and receptor-ligand separation [13,14]. Therefore, how to incorporate these effects into a kinetics model is worth studying. Third, only when receptors at the remote part of cell membrane are able to diffuse toward the adhesion front and arrive at close proximity to the substrate, can they interact with ligands and form specific adhesion. Hence the bond formation can be limited by the cell's ability to recruit receptors to the spreading front [11,12,15,16]. However, the role that the long-range force plays in the recruiting process has not been explicitly considered. Since the long-range force initiates the shallow adhesion of cell, it may also play an active role in recruiting remote receptors. Hence the effect of long-range force in recruiting remote receptors on the cell membrane needs to be considered in formulating cell adhesion model.

In this paper, we establish a continuum mechanics framework to model the adhesion of a cell to a substrate surface. The cell is modeled as a simplified cell structure, whose

*Corresponding author. FAX: 65 6776 3604; msezyw@nus.edu.sg

membrane is a cellular phospholipid bilayer doped with a controlled set of binder proteins and supported by a spectrin network [11]. A fluid of fixed volume is enclosed within the membrane. The ligands on the substrate are assumed to be uniform and fixed; while the mobile receptors on the cell membrane are uniformly distributed initially and may redistribute when subjected to long-range recruiting forces and specific interactions with the substrate. A traction-separation relation is used to describe the long-range recruiting interaction between the cell and the substrate, while a chemical reaction equation is adopted to describe the specific interaction between the receptors and ligands. A diffusion model is proposed to describe receptor movement within membrane driven by long-range recruiting force. Parametric studies will be performed to investigate the effects of the various system parameters on the spreading process.

II. MODEL FORMULATION

A. Long-range recruiting force

Long-range recruiting interaction between the cell and substrate is much weaker than the specific interaction. The long-range recruiting interaction may be a lump-sum effect of various types of forces, for example, attractive van der Waals forces and/or electrostatic forces [17]. Since mobile molecules on the membrane can diffuse within the membrane when subjected to external forces and concentration gradient, it is expected that these relatively long-range attractive forces will serve as a recruiting force for mobile molecules such as receptors to diffuse to the adhesion front.

In the present formulation, the long-range force plays an important role in recruiting the receptors on the membrane to diffuse toward the substrate and accumulate at the spreading front. To specify the range and magnitude of the long-range recruiting force, a traction separation relation was used [18,19]. For simplification, we adopt the following linear traction-separation relation to define the traction on receptors due to the long-range attractive interactions:

$$T_n = \begin{cases} 0 & \delta > \delta_c \\ H(\rho_r - \rho_b)\left(1 - \dfrac{\delta}{\delta_c}\right) & \delta \le \delta_c, \end{cases} \tag{1}$$

where ρ_r is the total receptor density, ρ_b is the density of receptor-ligand bonds, T_n is the traction force per unit area on the mobile receptors with a density of $\rho_r - \rho_b$, δ measures the separation between the receptors and the substrate, H is the long-range recruiting pulling force acting on a single receptor at the reference state $\delta=0$, and δ_c is the cut-off interaction distance beyond which the long-range recruiting force becomes negligible (see Fig. 1).

B. Specific interaction

Cell adhesion is mediated by specific interactions between receptors and ligands. The kinetics and mechanics of cell adhesion are coupled because specific interaction not only provides the mechanical load for cell-substrate adhesion but also strongly influences the dissociation rates of receptor-ligand bonds as well [3,4,10,13]. Studies on individual specific bonds tethered to solid surfaces have revealed that the dissociation rate of such bonds is drastically increased upon force application [3,4,13,20]. Besides, it was also shown recently that the distance between receptor and ligand is also an important parameter controlling the specific bond formation [14]. Based on these understandings, the following reaction equation is proposed for the receptor-ligand formation, that is, from the shallow adhesion state to the tight adhesion state,

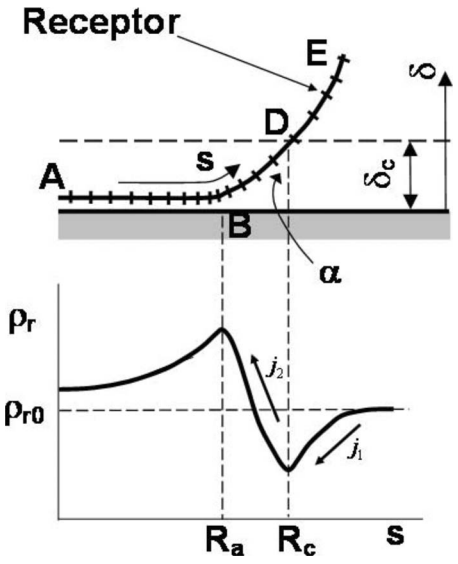

FIG. 1. Variation in receptor density caused by diffusion of the receptors on the cell surface. Receptors can diffuse from D to B due to the attraction of the adhesion forces and from E to D due to the receptor density gradient.

$$\frac{d\rho_b}{dt} = k_f(\rho_r - \rho_b)(\rho_l - \rho_b)e^{-(\delta/\delta_b)^2} - k_r\rho_b e^{\Gamma/\rho_b KT}, \tag{2a}$$

where ρ_l is the ligand density on the substrate surface, k_f and k_r are the forward and reverse reaction rate coefficients, respectively, δ_b is a characteristic length, which is related to the distance between the shallow adhesion state and the tight adhesion state and temperature, K is the Boltzmann constant, and T is the absolute temperature; Γ is the elastic energy density stored on local receptor-ligand bonds due to the specific traction T_s,

$$\Gamma = \frac{1}{2}T_s\delta,$$

$$T_s = \rho_b k_0 \delta, \tag{2b}$$

where k_0 is the stiffness of a single receptor-ligand bond.

C. Receptor diffusion on cell membrane

Both long-range recruiting forces and nonuniformly distributed density will result in receptor diffusion flux within a bilayer membrane. For the receptor diffusion caused by density gradient, the diffusion flux on the membrane surface is

$$j_\rho = -D\frac{\partial \rho_r}{\partial s}, \tag{3a}$$

where D is the receptor diffusivity on the membrane. For diffusion flux driven by the long-range recruiting force, it was assumed to be proportional to the traction tangential to the membrane surface, therefore

$$j_T = MT_n \cos(\alpha), \tag{3b}$$

where M is the receptor mobility in the membrane under the long-range recruiting force, $T_n \cos(\alpha)$ represents the tangential component of the traction. Thus, the total diffusion flux can be written as

$$j = j_T + j_\rho = MT_n \cos(\alpha) - D\frac{\partial \rho_r}{\partial s}. \tag{4}$$

Since the number of receptors in the lipid membrane is conserved, the governing equation for the receptor density is

$$\frac{\partial \rho_r}{\partial t} = \frac{\partial j}{\partial s} = M\frac{\partial [T_n \cos(\alpha)]}{\partial s} - D\frac{\partial^2 \rho_r}{\partial s^2}. \tag{5}$$

Consequently, ρ_r is a function of the time and location on the cell membrane surface. Its distribution during the spreading process is shown schematically in Fig. 1, where a portion of the cell membrane is assumed to have adhered to the substrate with point B at the adhesion front, point D at the cut-off front of the interaction force, and point E in the remote undisturbed zone. It is further assumed that the receptors in the adhered area AB are immobilized. The receptors in the adhesive zone BD would move along the arc BD toward point B under the attraction of the long-range recruiting forces which act downwards and had a tangential component along the arc BD. This consequently leads to a receptor density gradient in the zone DE, causing further recruitment of receptors from the undisturbed area toward cut-off front D.

D. Model formulation for cell structure and the substrate

In the present work, an incompressible Yeoh hyperelastic shell was chosen to model the composite layer of the lipid bilayer membrane and its supported spectrin network. The strain energy potential function is given by [21]

$$U = \frac{G}{2}(\lambda_1^2 + \lambda_2^2 + \lambda_3^2 - 3) + C_{30}(\lambda_1^2 + \lambda_2^2 + \lambda_3^2 - 3)^3, \tag{6}$$

where G is the initial bulk shear modulus and the parameter C_{30} is taken $C_{30}=G/30$ to best match experimental data [22]. λ_i $(i=1,2,3)$ are the principal stretches. If incompressibility is assumed, $\lambda_1\lambda_2\lambda_3=1$. The Yeoh hyperelastic potential is known to be reasonably accurate even when the maximum strain is of the order of 100% [22]. Previous studies have shown that the effect of membrane viscosity on cell deformation was negligibly small [22]. Therefore the membrane viscoelasticity was not accounted for in the present work.

The cytoplasm is idealized as an incompressible fluid [21]. For simplification, the fluid was assumed to be homogenous in composition and density. The fluid exerts a uniform pressure on the cell membrane. When the cell membrane deforms, the volume of cytoplasm remains constant but the pressure may change. The viscosity of the fluid can be ignored [22].

To simplify the model, the substrate to which the cell adheres was assumed to be rigid. Interpenetration of the membrane and the substrate surface was not allowed. It was further assumed that there was no friction between the membrane and the substrate surface.

III. SIMULATION MODEL AND NUMERICAL PROCEDURE

An axisymmetic finite element model was used to simulate the cell adhesion problem. The deformation of the cell was computed using a commercially available general purpose finite-element package ABAQUS [21]. The membrane was modeled by shell element. A user subroutine following ABAQUS regulations was coded to delineate the formation and dissociation of the receptor-ligand bonds. Hydrostatic fluid elements were used to analyze the mechanical response of the fluid-filled cavity. It should be noted that the finite element computation was a highly nonlinear static analysis due to the cell membrane hyperelasticity and contact interfaces. To ensure numerical stability of the solution, a small damping factor was introduced in the calculations.

The spreading process was simulated in an incremental manner in a number of steps. Each incremental step consists of two parts. In the first part, the traction forces acting on the cell surface were calculated and diffusion of the receptors on the membrane surface was analyzed. Finite element procedure was developed to solve this diffusion equation. These calculations were performed based on the current cell configuration. After the traction forces at all element nodes were obtained, the new receptor densities were computed. In the second part, the deformation of the cell under the long-range recruiting forces and the specific bond forces were analyzed on the ABAQUS platform, while ensuring that the contact condition was satisfied. The bond forces and bond density were computed in the abovementioned user subroutine at each iteration increment. The updated cell shape and densities of the receptors were then utilized for the next step. As the simulation proceeds step by step, the cell spreads on the substrate in response to the long-range recruiting force and specific tractions until the deformation and receptor diffusion reached equilibrium without net receptor flux on the membrane and without further increase in the adhesion area. The analysis is therefore terminated.

The values of typical parameters of our model for biological systems were chosen based on previous works [22–24]: the shear modulus of cell wall $G=6$ kPa and the thickness of cell wall $h=20$ nm; the cell radius $R_0=3.1$ μm; the long-range force coefficients $H=1$ pN and $\delta_c=0.1$ μm; the bond rupture/rebinding parameters $k_f=10^{-1}$ $\mu m^2/s$, $k_r=10^{-5}/s$, $k_0=10^{-3}$ N/m, and $\delta_b=0.01$ μm; the receptor diffusivity $D=10^{-3}$ $\mu m^2/s$ and mobility $M=2.5\times10^5$ $\mu m/\mu N\cdot s$; the ligand density $\rho_l=5000$ μm^{-2} and initial receptor density $\rho_{r0}=300$ μm^{-2}; the diffusion time step $\Delta t=10$ ms. The initial configuration is chosen as a spherical cell with a uniform distribution of receptors on its surface making a point contact

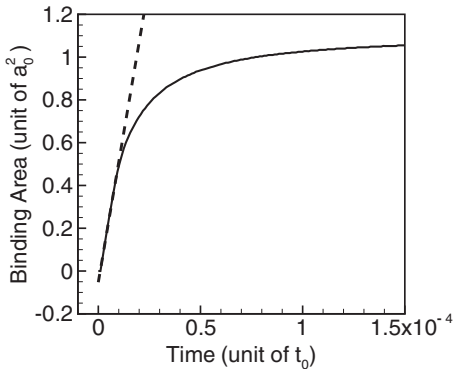

FIG. 2. The curve of binding area vs spreading time for the typical case ($H=1$ pN and $\delta_c=0.1$ μm; $k_f=10^{-1}$ μm^2/s, $k_r=10^{-5}$/s, and $\delta_b=0.01$ μm). The fitting at the early stage (dashed line) shows a scale of $a^2 \propto t$, which is consistent with the theoretic prediction.

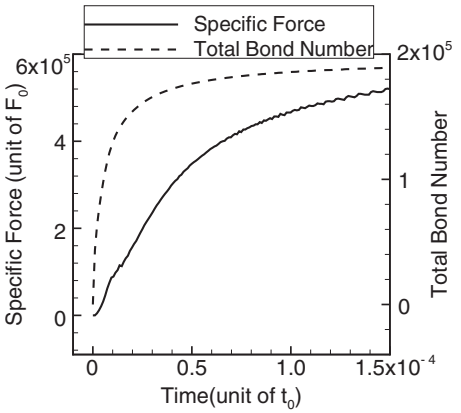

FIG. 3. The curves of total normalized specific forces (solid line) and the total number of receptor-ligand bonds (dashed line) vs spreading time for the typical case.

with a flat surface covered by a uniform and fixed distribution of ligands.

Our simulation results were reported using the following normalization scheme: length was normalized by the diameter of the cell, i.e., $a_0=D_0$; time by $t_0=a_0^2/D$, energy by $E_0=KT_R$, where K is Boltzmann constant and T_R is the room temperature; force by $F_0=E_0/a_0$.

IV. RESULTS

A. Simulation results for the typical case

Figure 2 shows the spreading kinetics for the typical case. Initially, there is no specific adhesion, and the binding starts from a small contact area with shallow adhesion mediated by long-range recruiting force between the cell and the substrate. At the early stage, the specific force increases rapidly due to the rapid increase in receptor-ligand bond number. Subsequently, the binding area growth levels off and gradually stabilizes at equilibrium state. The equilibrium is achieved only when no net diffusion fluxes occur on the surface and the reaction to form receptor-ligand bonds reaches steady state.

The adhesion of a biomimetic cell onto a solid substrate was studied previously [11,25]. When the coverage of receptors on the cell is much lower than ligands on the substrate, which is the case in our present model, it was found that the spreading front motion following the square root law $a \propto \sqrt{t}$, namely, $a^2 \propto t$, where a is the radius of the binding area and t is the spreading time. In a subsequent experimental study [9], a similar power law $a \propto t^n$ was obtained with an exponent $n=0.48 \pm 0.06$. It was recognized that this square root law is only valid when the receptor-ligand bond formation is much faster than receptor diffusion on the membrane; otherwise the exponent drops down to $n=0.27 \pm 0.04$ [9]. However, none of these observations exactly match our results. It is found that in Fig. 2, only the initial part of the curve can be fitted by the linear relation between the binding area and the spreading time ($a^2 \propto t$). Subsequently the exponent levels off in the later stages. In the present model, both the cell size and the number of receptors available for forming bonds are finite. This limitation hinders the growth of binding area as the spreading proceeds. Consequently, the cell adhesion will necessarily come to saturation eventually. Hence this difference is attributed to the finite-size effect. Figure 3 shows the normalized specific force and the receptor-ligand bond number varying with time in the whole spreading process. It is evident that once the cell approached the substrate, specific force was built up due to the substantial increase in the receptor-ligand bond density.

B. Parametric studies of system parameters

To further understand how cell spreading kinetics depends quantitatively and qualitatively on system parameters, we perform parametric studies to investigate the influence of system parameters. In our parametric studies, typical values of the system parameters were employed unless stated otherwise.

1. Effects of long-range recruiting force parameters H and δ_c

Figures 4 and 5 show the normalized binding area as a function of spreading time at different values of H and δ_c, respectively. It is seen that increasing either H or δ_c leads to an increase in spreading rate and binding area. However, the

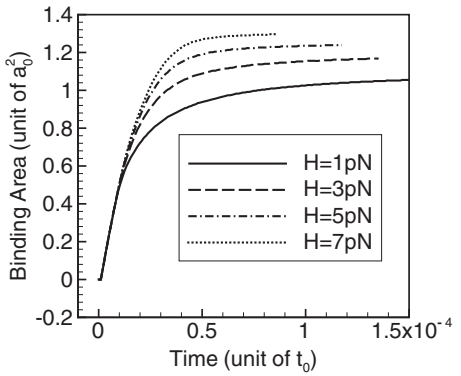

FIG. 4. The curves of binding area vs spreading time at different values of the long-range recruiting force coefficient H.

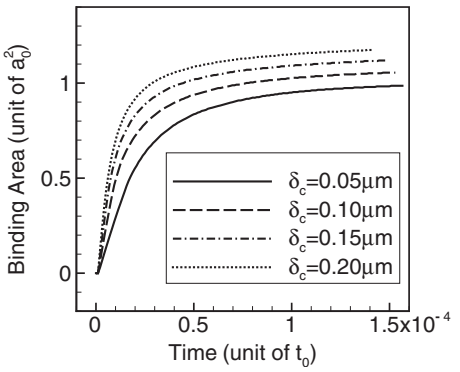

FIG. 5. The curves of binding area vs spreading time at different values of the long-range recruiting force cut-off distance δ_c.

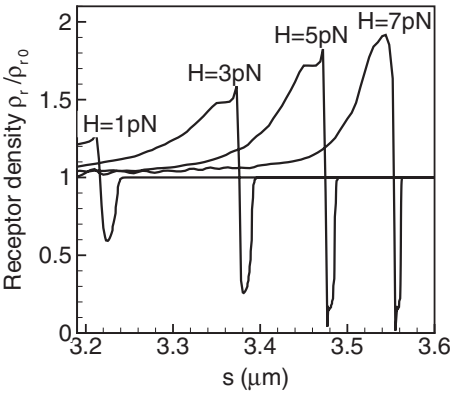

FIG. 6. Distribution of the normalized receptor density (ρ_r/ρ_{r0}) along the normalized arclength (s/a_0) at the final stage of spreading with different H.

curves overlap at the initial stage and tend to saturate when H increases (see Fig. 4), whereas these two characteristics are absent when varying δ_c (see Fig. 5). This can be explained by the different influences of these two parameters at different spreading stages. In the initial adhesion, δ_c determines the size of the zone under long-range recruiting force, while H affects the strength of this force. It is obvious that the effect of δ_c is significant from the very beginning, while the effect of H is not apparent, that is, the curves at different values of H overlap at the initial stage. In the subsequent adhesion (dominated by specific force), δ_c determines the size of the membrane region within which the receptors are under the long-range recruiting force, thus can be pulled down toward to the adhesion front to form bonds. The coefficient H controls the magnitude of this pulling force. Increasing H implies an elevated receptor influx, and hence an accelerated bond formation and spreading velocity. However when H is too large, its influence becomes less significant, which means that other factors emerge to control the adhesion.

As shown in Fig. 1, there could be three kinetic processes for the cell adhesion: (1) the receptor diffusion flux driven by the receptor concentration gradient, $j_1=-D\frac{\partial \rho_r}{\partial s}$; (2) the receptor diffusion flux driven by the long-range recruiting forces, $j_2=MT_n\cos(\alpha)-D\frac{\partial \rho_r}{\partial s}$; and (3) the bond formation rate at the adhesion front controlled by $\frac{d\rho_b}{dt}=k_f(\rho_r-\rho_b)(\rho_l-\rho_b)e^{-(\delta/\delta_b)^2}-k_r\rho_b e^{\Gamma/\rho_b KT}$. The slowest process among them will be the major limiting factor to the adhesion.

Figure 6 displays the receptor density distribution along the cell arclength at the late stage of spreading. It is seen that when H rises to 5 pN, the receptor density at the cut-off position of the long-range recruiting force drops to nearly 0, indicating that receptors are already drained out at this position. This happens because when H is too high, the receptor influx to the adhesion front j_2 is so high that there would not be adequate time for receptors to diffuse to the cut-off front to compensate for the reduction in receptor concentration. Therefore, it can be concluded that the saturation observed for high values of H results from the limitation of j_1, that is, the receptor diffusion from the undisturbed zone to the adhesive zone.

2. Effects of forward reaction rate coefficients k_f and δ_b

Both k_f and δ_b directly affect the forward rate of bonding reaction. The coefficient k_f influences the maximum value of the rate, while the characteristic length δ_b determines the range within which the bond formation will most likely happen.

Figure 7 shows the binding area as a function of spreading time for different values of k_f. It is observed that a change in k_f from 0.01 to 0.2 $\mu m^2/s$ leads to an obvious increase in both the spreading velocity and binding area. The change in spreading kinetics is remarkable as k_f increases from 0.01 to 0.1 $\mu m^2/s$. The curve for $k_f=0.01$ $\mu m^2/s$ exhibits a much weak power law compared to the other two. This is a regime limited by the bond formation rate (reaction-limited regime), a case reminiscent of the observations in [9]: as the binding rate is no longer much faster than diffusion time, the spreading front motion displays a power law with exponent $n=0.27\pm0.04$. Beyond 0.1 $\mu m^2/s$, the change in spreading kinetics is attenuated as k_f is further increased, which means that the limiting factor that dominates the adhesion has shifted from the bond formation rate to diffusion fluxes (either j_1 or j_2 as shown Fig. 1). By plotting the receptor distribution for different k_f at the late stage in Fig. 8, we found that there were still enough free receptors at the cut-off location. Therefore, it is concluded that the diffusion influx j_2 limits the adhesion at high values of k_f. When k_f is too large, that is, the bond formation rate is so high that there will not be enough time for free receptors to move from the cut-off location to compensate for the reduced receptor concentra-

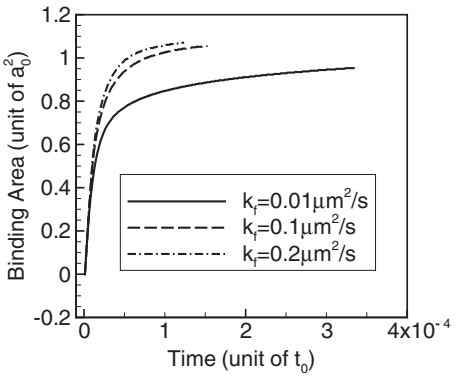

FIG. 7. The curves of binding area vs spreading time at different values of the forward reaction rate coefficient k_f.

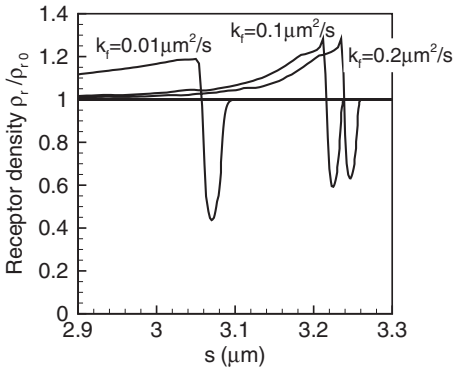

FIG. 8. Distribution of the normalized receptor density (ρ_r/ρ_{r0}) along the normalized arclength (s/a_0) at the final stage of spreading with different values of k_f.

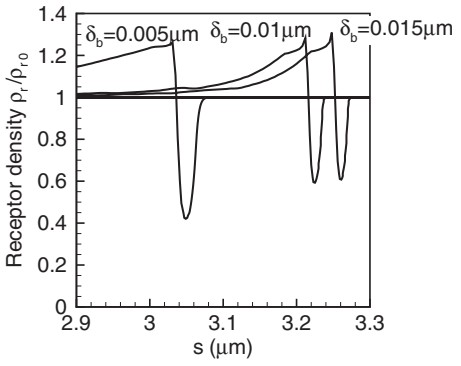

FIG. 10. Distribution of the normalized receptor density (ρ_r/ρ_{r0}) along the normalized arclength (s/a_0) at the final stage of spreading with different values of δ_b.

tion at the adhesion front. As a consequence, saturation was obtained.

Figure 9 shows the binding area as a function of spreading time at different δ_b, where δ_b is the characteristic length, within which the probability of bond formation is close to 1, while beyond which this probability drops to 0 rapidly; Thus similar to k_f, an increase in δ_b effectively facilitates the receptor consumption at the spreading front. Therefore the curves in Fig. 9 display the same trends as δ_b increases, and saturation was also observed at higher values of δ_b. To elucidate the limiting factor which causes the saturation, we plotted the receptor distribution at different values of δ_b at the late spreading stage in Fig. 10. It is shown that the valley point at the long-range recruiting force cut-off position is still larger than 0. This implies that it is the limitation of the diffusion influx j_2 that causes the saturation for high values of δ_b, similar to the limiting effect of k_f.

3. Effects of reverse reaction rate coefficient k_r

It was shown that when the receptor-ligand bonds are under stress, their lifetime may be decreased [13]. Therefore, a reverse reaction rate was introduced in the present model, and the rate has a base value of k_r when a receptor-ligand bond is free of stress. Figure 11 shows the binding area as a function of spreading time for several different values of k_r. An order of increase in k_r gives rise to a less than 5% decrease in the binding area. The insignificant change reveals that during the spreading process, bonds are just slightly stressed. Therefore the effect of reverse reaction rate is insignificant. However, in the peeling and pulling test, it is expected that the reverser reaction rate would play an important part in controlling the cell unbinding kinetics [13,26–29].

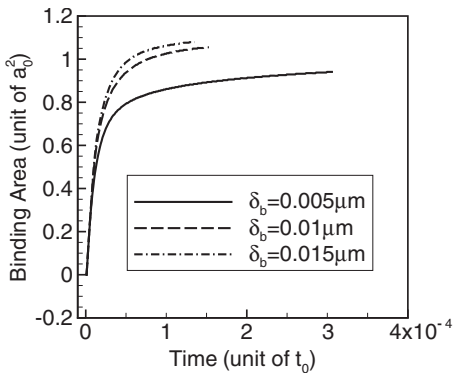

FIG. 9. The curves of binding area vs spreading time at different values of the specific characteristic length δ_b.

V. DISCUSSION and CONCLUSIONS

Adhesion of cells to the extracellular matrix has been extensively explored by both experimental studies and theoretical models. Different spreading kinetics were proposed between the adhesion area and the spreading time under different conditions [11,12,30]. Experiments also showed different spreading kinetics under very different cell types and receptor and ligand details [9].

In the present work, a simplified cell system model was employed to reveal rich kinetic phenomena in the study of cell adhesion. A continuum modeling framework has been established. Several refinements have been made over the previous models. First, long-range recruiting force and the specific interaction have been separated based on their very different natures and functions. Second, finite-size effects of the cell and the number of receptors were included. Finally, a

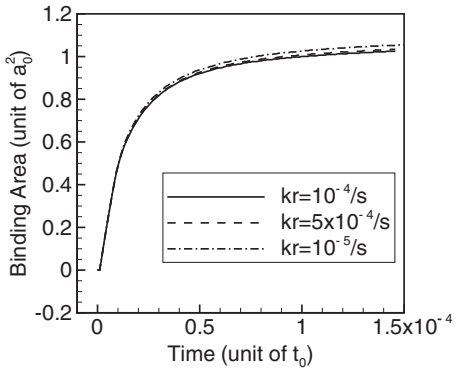

FIG. 11. The curves of binding area vs spreading time at different values of the reverse reaction rate coefficient k_r. It is seen that the effect of reverse reaction rate coefficient k_r is insignificant.

chemical reaction equation was introduced to describe the bonding and debonding events between receptors and ligands. Effects of both the interfacial stress and receptor-ligand separation were considered. The results of the calculations exhibited different spreading stages mediated by different mechanisms and revealed different distinct regimes in which adhesion is limited by different mechanisms. By introducing the recruiting role of long-range attractive forces, we demonstrated three possible limiting regimes for the cell adhesion: (1) the receptor concentration gradient driven diffusion limited regime, (2) the long-range recruiting force driven diffusion limited regime, and (3) the bond formation rate limited regime. Among them the slowest process will be the major limiting factor to the adhesion. The relative magnitude of the three parameters, that is, D, H, and k_f, controls which process is the limiting one. Our simulations have shown that when D is small, while other remaining two are large, the receptor concentration gradient driven diffusion will be the limiting process. When H is small while other remaining two are large, the long-range recruiting force driven diffusion will be the limiting case. When k_f is small while other remaining two are large, the bond formation process is the limiting one. It is also shown that the effect of the reverse reaction rate k_r is insignificant due to lower stress state for receptor-ligand bonds.

To model the more realistic situation in cell adhesion, several issues still need to be addressed. First, the present long-range recruiting force takes a very simple form, thus may not describe the actual form for the long-range recruiting force. A double-minimum free-energy model was proposed and was attested experimentally [3,4]. How to incorporate this double-minimum free-energy model into the present model would be an interesting research issue. Second, the actively driven cytoskeletal remodeling is in need of consideration. The present simulations only describe the early stages of cell adhesion, while in longer time scales, the actin cytoskeleton couples to the adhesion domains, leading to a cascade of intracellular signaling events and the formation of focal adhesion. This suggests that the nature and strength of the cell-substratum interactions may also involve activities of the cell cytoskeleton [2,31–35]. Third, in our present work, the traditional composite structure for the cell membrane is assumed and represented by the shell theory [36,37]. It is understood that alternative models were also proposed and suggested a sparse connection between the lipid bilayer and spectrin network [38,39]. Under this condition, the cytoskeleton-membrane structure may not be reasonably treated as a composite layer with a finite shear modulus. Therefore, the model accounting for the mechanical properties of cell membrane is still an issue of debate. Fourth, membrane fluctuation needs to be taken into account. Numerous studies have revealed the importance of membrane fluctuation in cell adhesion processes. For example, it can induce a membrane protein segregation [40,41], and it can also influence the nucleation and the effective binding affinity of cells [42,43]. Hence how to incorporate membrane fluctuation into the present continuum model is an important future work.

ACKNOWLEDGMENTS

This work was supported by Academic Research Fund (Grant No. R-284-000-055-112) through the Faculty of Engineering, National University of Singapore.

[1] G. Bao and S. Suresh, Nature Mater. **2**, 715 (2003).
[2] C. W. Wolgemuth, Biophys. J. **89**, 1643 (2005).
[3] G. I. Bell, Science **200**, 618 (1978).
[4] G. I. Bell, M. Dembo, and P. Bongrand, Biophys. J. **45**, 1051 (1984).
[5] E. Zamir and B. Geiger, J. Cell Sci. **114**, 3583 (2001).
[6] N. Q. Balaban, U. S. Schwarz, and D. Riveline, Nat. Cell Biol. **3**, 466 (2001).
[7] A. D. Bershadsky, N. Q. Balaban, and B. Geiger, Annu. Rev. Cell Dev. Biol. **19**, 677 (2003).
[8] C. A. Reinhart-King, M. Dembo, and D. A. Hammer, Biophys. J. **89**, 676 (2005).
[9] D. Cuvelier and P. Nassoy, Phys. Rev. Lett. **93**, 228101 (2004).
[10] E. A. Evans, Biophys. J. **48**, 175 (1985).
[11] A. Boulbitch, Z. Guttenberg, and E. Sackmann, Biophys. J. **81**, 2743 (2001).
[12] V. B. Shenoy and L. B. Freund, Proc. Natl. Acad. Sci. U.S.A. **102**, 3213 (2005).
[13] M. Dembo, D. C. Torney, K. Saxman, and D. A. Hammer, Proc. R. Soc. London, Ser. B. **234**, 55 (1988).
[14] T. Erdmann and U. S. Schwarz, Eur. Phys. J. E **22**, 123 (2007).
[15] H. J. Gao, W. Shi, and L. B. Freund, Proc. Natl. Acad. Sci. U.S.A. **102**, 9469 (2005).
[16] P. Liu, Y. W. Zhang, Q. H. Cheng, and C. Lu, J. Mech. Phys. Solids **55**, 1166 (2007).
[17] D. E. Leckband, J. N. Israelachvili, F. J. Schmitt, and W. Knoll, Science **255**, 1419 (1992).
[18] V. Tvergaard and J. W. Hutchsinson, J. Mech. Phys. Solids **41**, 1119 (1993).
[19] P. Liu, L. Cheng, and Y. W. Zhang, Acta Mater. **49**, 817 (2001).
[20] E. L. Florin, V. T. Moy, and H. E. Gaub, Science **264**, 415 (1994).
[21] ABAQUS User's Manual, Version 6.7 (ABAQUS Inc., Pawtucket, RI, 2007).
[22] J. P. Mills, L. Qie, M. Dao, C. T. Lim, and S. Suresh, Mech. Chem. Biosyst. **1**, 169 (2004).
[23] S. Pierrat, F. Brochart-Wyart, and P. Nassoy, Biophys. J. **87**, 2855 (2004).
[24] J. J. Valle-Delgado, J. A. Molina-Bolivar, F. Galisteo-Gonzalez, M. J. Galvez-Ruiz, A. Feiler, and M. W. Rutland, Langmuir **22**, 5108 (2006).
[25] L. B. Freund and Y. Lin, J. Mech. Phys. Solids **52**, 2455 (2004).
[26] D. A. Hammer and D. A. Lauffenburger, Biophys. J. **52**, 475 (1987).
[27] C. Zhu, G. Bao, and N. Wang, Annu. Rev. Biomed. Eng. **2**,

189 (2000).
[28] Y. S. Chu, S. Dufour, J. P. Thiery, E. Perez, and F. Pincet, Phys. Rev. Lett. **94**, 028102 (2005).
[29] A. S. Smith and U. Seifert, Phys. Rev. E **71**, 061902 (2005).
[30] D. Cuvelier, M. Théry, Y. S. Chu, S. Dufour, J. P. Thiéry, M. Bornens, P. Nassoy, and L. Mahadevan, Curr. Biol. **17**, 694 (2007).
[31] B. J. Dubin-Thaler, G. Giannone, H. G. Dobereiner, and M. P. Sheetz, Biophys. J. **86**, 1794 (2004).
[32] J. L. Tan, J. Tien, D. M. Pirone, D. S. Gray, K. Bhadriraju, and C. S. Chen, Proc. Natl. Acad. Sci. U.S.A. **100**, 1484 (2003).
[33] D. Boal, *Mechanics of the Cell* (Cambridge University Press, New York, 2002).
[34] A. J. Engler, S. Sen, H. L. Sweeney, and D. E. Discher, Cell **126**, 677 (2006).
[35] D. J. Irvine, K. A. Hue, A. M. Mayes, and L. G. Griffith, Biophys. J. **82**, 120 (2002).
[36] G. Karp, *Cell and Molecular Biology: Concept and Experiments* (John Wiley & Sons, New York, 2008).
[37] E. A. Evans and R. Skalak, *Mechanics and Thermodynamics of Biomembranes* (CRC Press, Boca Raton, FL, 1980).
[38] N. Gov, A. G. Zilman, and S. Safran, Phys. Rev. Lett. **90**, 228101 (2003).
[39] S. A. Safran, N. Gov, A. Nicolas, U. S. Schwarz, and T. Tlusty, Physica A **352**, 171 (2005).
[40] T. R. Weikl, J. T. Groves, and R. Lipowsky, Europhys. Lett. **59**, 916 (2002).
[41] T. R. Weikl, Europhys. Lett. **54**, 547 (2001).
[42] D. Coombs, M. Dembo, C. Wofsy, and B. Goldstein, Biophys. J. **86**, 1408 (2004).
[43] E. Reister-Gottfried, K. Sengupta, B. Lorz, E. Sackmann, U. Seifert, and A. S. Smith, Phys. Rev. Lett. **101**, 208103 (2008).